International Journal of Biological Macromolecules 319 (2025) 145497

Contents lists available at ScienceDirect

International Journal of Biological Macromolecules

journal homepage: www.elsevier.com/locate/ijbiomac

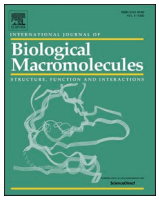

Enhancing the thermal stability and activity of the engineered self-sufficient P450$_{SP\alpha}$-SOX by switching the domains linker

Daniele Giuriato, Gianluca Catucci, Danilo Correddu, Gianfranco Gilardi *

Department of Life Sciences and Systems Biology, University of Torino, Via Accademia Albertina 13, 10123, Torino, Italy

ARTICLE INFO

Keywords:
Molecular Lego
Engineered linker
P450 SPα
Sarcosine oxidase
H_2O_2 generation
Styrene
Fusion enzyme
Differential scanning calorimetry

ABSTRACT

This work reports on the engineering of the linker between P450 SPα (CYP152B1) and sarcosine oxidase (SOX), with the aim of enhancing the structural rigidity of the fusion protein (SPα-SOX) and study the effect on its stability and catalytic performance. Differential scanning calorimetry shows that the construct bearing the rigid linker (SPα-rigid-SOX) results in a higher energy barrier to unfolding (765 kcal/mol) compared to the previous fusion system (SPα-flexible-SOX) (561 kcal/mol), as well as a T_{onset} above 50 °C. Furthermore, residual CO-binding after heat treatment was investigated for both the fusion systems, and a 5.7 °C increase of the T_{50} of SPα-rigid-SOX is shown. Interestingly, a stabilized P420 semi-folded state of the SPα is also observed after SPα-rigid-SOX incubation at high temperature (40°). The two fusion systems were studied at high temperature for the turnover of lauric acid: SPα-rigid-SOX shows a 98 % conversion yield using 5 mM substrate compared to the 24 % conversion of SPα-flexible-SOX when the catalysis is carried out at 40 °C. Finally, the activity of the two constructs was tested using styrene as a substrate, and three products of catalysis were observed: styrene oxide (85 %), phenylacetaldehyde (0–3 %) and 2-phenylpropenal (12–15 %). Interestingly, 2-phenylpropenal is observed for the first time and only for the fusion enzymes. Also in this case, SPα-rigid-SOX outperformed SPα-flexible-SOX with a 3-fold higher conversion yield. Overall, we demonstrate that the rigid linker improves the fusion enzyme thermal stability and catalytic performance, both at high temperature and in mild conditions, resulting also in the production of new molecules of biotechnological interest.

1. Introduction

The exploitation of enzymes as industrial biocatalysts is appealing but often unfeasible because of their relatively low turnover and poor stability. In particular, cytochromes P450 are interesting for their broad range of reaction specificity, regio- and stereo-selectivity. Unfortunately, the majority of these enzymes needs NAD(*P*)H to drive their catalysis, which represents a limitation for their extensive economically viable exploitation as biocatalysts [1]. Where possible, a widely used approach is to exploit the peroxygenase activity of some P450s, avoiding the economic and technical limitation of the use of redox partners [2]. However, also in this case the intrinsic toxicity of hydrogen peroxide toward proteins, as well as its limits of compatibility with cellular life, goes to limit the large-scale exploitation of this approach. Protein engineering allows to design artificial fusion proteins, to be efficiently used in biocatalytic cascades and to increase the catalytic performance of several class of enzymes [3–8]. Fusion proteins are powerful tools to combine two or more enzyme functionalities in a cascade reaction, while at the same time increasing the stability and catalytic performance of the fusion system [9]. Artificial fusion proteins are engineered by recombining two or more genes that originally encode separated proteins, possibly even from different organisms. By the *Molecular Lego* approach, multidomain enzyme "chimeras" are engineered to include two non-physiological partner enzymes joined together in a single polypeptide chain [10,11]. The proximity of the binding pockets of the two enzyme in the fusion protein optimizes the transfer of the metabolic intermediate between the active sites of the two catalytic partners, minimizing their diffusion in solution, that often represents one of the rate-limiting steps in the cascade reactions [3,5,12]. A crucial aspect addressed when optimizing fusion proteins engineering, is the physical-chemical properties of the linker peptide that connects the different enzymes. A fusion enzyme linker is defined by its peptide sequence, which leads to diverse secondary structures - usually α-helixes or disordered loops - but also its length, flexibility or rigidity and orientation [5,12]. In this work, the development of two fusion enzymes functioning as artificial self-sufficient peroxygenases is presented. Previously, we reported on a

* Corresponding author.
E-mail address: gianfranco.gilardi@unito.it (G. Gilardi).

https://doi.org/10.1016/j.ijbiomac.2025.145497
Received 15 April 2025; Received in revised form 13 June 2025; Accepted 23 June 2025
Available online 23 June 2025

SPα-SOX fusion enzyme able to self-regenerate hydrogen peroxide sustaining the conversion of fatty acids in α-hydroxy fatty acids by the peroxygenase activity of the P450 SPα [13]. It was proved that not only the sarcosine-driven self-sufficient catalysis of the fusion enzyme outperformed the isolated wild type SPα enzyme [14,15], but the stability of the enzyme toward the hydrogen peroxide was also improved, thanks to the ability to modulate its in-situ production by the SOX domain activity. Encouraged by these results, in this work the design of the biocatalyst is optimized by finely tuning the properties of the linker sequence between the two enzymatic domains – the SPα and the SOX domain. We designed a new construct with a different domains-linker sequence (EPPPPLPPPPE), that is meant to confer a higher structural rigidity compared to the previous construct. For this reason, the two constructs have been named SPα-flexible-SOX and SPα-rigid-SOX. The effect of the linker rigidity on the physical-chemical properties of the enzyme was investigated in terms of unfolding process by calorimetry, UV-VIS spectroscopy, activity, and performance at high temperature (40 °C).

2. Methods

2.1. Structure prediction

AlphaFold 2.0 [16] was used to predict the 3-D structure of SPα-rigid-SOX and SPα-flexible-SOX. The two proteins models' energy was minimized using YASARA energy minimization tool. The resulting structures were analyzed using MolProbity Ramachandran analysis [17,18] to extrapolate the ϕ and ψ main chain torsion angles.

2.2. Enzymes preparation

The plasmid harboring the sequence of SPα-rigid-SOX was constructed as previously reported for that of SPα-flexible-SOX. [13] In brief, the SPα-rigid-SOX coding sequence (5′-3′) was designed by fusing the P450 152B1 sequence (PDB: 3VM4) [19], *Avr*II restriction site, the 33 nucleotides sequence coding for the domains linker (GAGCCGCCGCCGCCGCTGCCGCCGCCGCCGGAA), a *Asc*I restriction site, the SOX sequence (PDB: 2GB0) [20] and a 6xHis tag coding sequence. The SPα-rigid-SOX gene was inserted into a pET-28-a(+) expression vector by GenScript (Piscataway, NJ, USA) using the *Nco*I/*Eco*RI cloning strategy. The pET plasmids, harboring the SPα-flexible-SOX and the SPα-rigid-SOX genes, were used to transform *E. coli* BL21 (DE3) cells by heat shock. The transformed bacteria were grown at 37 °C in Terrific broth (TB) medium and selected with 50 μg/mL Kanamycin. After the optical density at 600 nm reached 0.4–0.6, the culture temperature was lowered to 20 °C, 0.5 mM δ-aminolevulinic acid and 50 μg/mL riboflavin was added. The protein expression was induced by adding 0.125 mM IPTG and carried out for 24 h at 20 °C. The cells were harvested by centrifugation at 4 °C, resuspended and sonicated (5 × 30 s pulses using a Misonix Ultrasonic Sonicator, Teltow, Germany) in 50 mM KPI at pH 7.4 supplemented with, 1 % Triton X-100, 20 mM imidazole, 1 mg/mL lysozyme, 0.1 mg/mL DNAse I, 1,5 mM PMSF. After 50 min ultracentrifugation at 45000 rpm, the soluble fraction of cell lysate was loaded into 5 ml nickel-ion affinity column (His-trap HP, GE Healthcare) hold at 8 °C. The column was washed with 20 column volumes of a solution containing 50 mM KPi at pH 7.4 supplemented with 75 mM imidazole and the target bounded protein was then eluted with 200 mM imidazole. The purified protein pools were loaded on a PD-10 Desalting Columns packed with Sephadex G-25 resin (Cytiva) to remove imidazole and exchange buffer and stored at −20 °C in 50 mM KPi pH 7.4, 200 mM KCl, 20 % glycerol. The pGEX-AX2 vector harboring a GST-tagged SPα gene was kindly gifted by Professor Yoshihito Watanabe laboratory. The isolated P450 SPα was expressed and purified as previously reported [21]. Protein purity was assessed by SDS-PAGE and the active protein fraction was quantified basing on the P450 form of SPα (ε_{445nm}: 91000 M^{-1} cm^{-1}) after reduction with sodium dithionite and pure carbon monoxide bubbling.

2.3. Differential scanning calorimetry

Microcal VP-DSC instrument (Malvern) was used to perform the differential scanning calorimetry analysis of SPα-rigid-SOX. The protein sample was suspended in 50 mM KPi at pH 7.4 supplemented with 10 % glycerol at a final concentration of 5 μM, the same buffer was used also for the reference scan. After 10 min of pre-scan equilibration the sample was analyzed applying a temperature gradient of 25–90 °C with a scan rate of 60 °C/h [10,13,22,23]. Data were analyzed using Microcal Origin software.

2.4. Heme domain residual activity: CO-binding assay

Protein samples containing 0.2 μM of either SPα-flexible-SOX or SPα-rigid-SOX were incubated in KPi solution at pH 7.4 at a scalar temperature of 30, 35, 40, 45, 50, 55, 60 or 65 °C for 20 min. Then each sample was analyzed using a Agilent 8453 UV–VIS spectrophotometer equipped with a Peltier Agilent 89,090 A. During the UV-VIS spectroscopy measurement the temperature was maintained at 25 °C. A first spectrum of the oxidized form of each enzyme was recorded, then excess of sodium dithionite was added and samples were bubbled with pure carbon monoxide for 30 s and the spectrum of the CO-bound form of the enzyme was recorded. The spectrum of the oxidized form of each sample was subtracted to the corresponding spectrum of the CO-bound form to obtain the difference spectra. In order to calculate the heme domain residual activity of each enzyme the absorbance at 445 nm of each sample was compared to that of an identical sample kept at 4 °C until the measurement (not pre-incubated at each temperature). All the experiments were performed in triplicate. The resulting data were plotted against temperature and the obtained curves were fitted to a sigmoidal Hill's like equation in four parameters:

$$f = \frac{y_0 + ax^b}{c^b + x^b}$$

where c is the T_{50} and b is the K_{decay}.

2.5. SOX residual activity: hydrogen peroxide production quantification

Protein samples containing 10 nM of either SPα-flexible-SOX or SPα-rigid-SOX were incubated in KPi solution at pH 7.4 at 46.5, 52.2 or 60 °C for 20 min. After that, the production of hydrogen peroxide was measured exploiting the HPR coupled reaction as previously described [7,13,24]. Samples were transferred in a NUNC96 96-well microplate (Thermo Fisher, MA, USA) and mixed with 0.42 μM horseradish peroxidase (HRP) and 208 μM ABTS. All reactions were performed in triplicate. The reaction was initiated by adding 42 mM sarcosine (reaching a final enzyme concentration of 7.5 nM) and the $ABTS^{\bullet+}$ production was monitored over 60 s by recording the absorbance at 420 nm every 5 s using a SPECTROstar nano microplate reader (BMG labtech, Aylesbury, UK). In order to calculate the SOX domain residual activity, the rate of $ABTS^{\bullet+}$ production of each sample was compared to that of an identical sample kept at 4 °C until the measurement (not pre-incubated at each temperature).

2.6. Lauric acid reactions

Lauric acid conversion reactions were carried out at either 30 or 40 °C. 1 μM of either P450 SPα, SPα-flexible-SOX or SPα-rigid-SOX was mixed in KPi buffer 50 mM at pH 7.4 supplemented with 5 % ethanol as cosolvent and 5 mM lauric acid. Wild type SPα reaction was started by the addition of 5 mM hydrogen peroxide. SPα-flexible-SOX and SPα-rigid-SOX reactions were started by the addition of 500 mM sarcosine. All reactions were performed in triplicate. After 1 h incubation at the

given temperature, reactions were extracted with 100 % vol/vol methyl tert-butyl ether (MTBE) and centrifuged 5 min at 12500 *g* to remove the denatured protein. The organic phase was transferred to a clean tube, diluted 1:10 in MTBE and derivatized adding 20 % vol/vol *N*,*O*-bis(trimethylsilyl)trifluoroacetamide with trimethylchlorosilane and incubating for 1 h at 50 °C. GC–MS measurements were performed using a Shimadzu single quadrupole GCMS–QP2020 NX equipped with a SH–I–5MS capillary column (30 m × 0.25 mm × 0.25 μm). Helium was used as a carrier gas with a flow of 1.85 mL min^{-1} and the injector temperature was set to 250 °C. Oven temperature was kept at 70 °C for 2 min, then it was raised at 15 °C min^{-1} up to 300 °C and held for 5 min. Mass spectra were collected using electrospray ionization (Fig. S1).

2.7. Styrene reactions

Fusion enzyme was diluted at a final concentration of 4 μM in 50 mM KPi at pH 7.4 supplemented with 500 mM sodium acetate, 10 % ethanol and respectively 0.5, 1, 2, 3, 6, 8 and 10 mM styrene. The SPα-rigid-SOX and SPα-flexible-SOX reactions were initiated by adding 500 mM sarcosine and carried out for 20 min at 30 °C. All reactions were performed in triplicate. The formaldehyde accumulated by SPα-SOX was quantified using a Formaldehyde Assay Kit (Sigma-Aldrich, St. Louis, MO 63103 USA), following the same method as previously described [7]. The wild type SPα reaction was performed using 5 μM enzyme, 10 mM styrene, 500 mM sodium acetate, 5 mM hydrogen peroxide and either 0, 2 or 5 mM of formaldehyde and carried out at 30 °C. After 20 min incubation the enzyme was inactivated and reaction products extracted. For the qualitative analysis of the metabolites production the reaction condition containing 10 mM styrene was extracted with 100 % vol/vol MTBE, the sample was centrifuged 5 min at 12500 *g* to remove the denatured protein, the organic phase was then transferred to a clean tube and diluted 1:2 in MTBE before analysis. The analysis was performed by GC–MS using a Shimadzu single quadrupole GCMS-QP2020 NX equipped with a SH-I5MS capillary column. Helium was used as a carrier gas with a flow of 1.17 mL min^{-1} and a split ratio of 10. The injector temperature was set to 250 °C. The oven temperature was set to 40 °C for 2 min then a first temperature ramp of 40–180 °C was applied at 10 °C min^{-1}. A second temperature ramp of 180–280 °C was applied at 40 °C min^{-1} and the temperature held for 1 min. Mass spectra were collected using electrospray ionization. For the study of the enzyme activity, reaction samples were stopped with 100 % ethanol, vortexed 30 s and centrifuged 5 min at 12500 *g* to remove the denatured protein. Styrene metabolites were separated and quantified using Agilent-1200 HPLC system equipped with a diode array UV detector and a ZORBAX C18 prepacked column (Agilent technologies, Santa Clara, CA, USA). The diode was set to 210 nm with 360 nm correction (Fig. S3). Styrene and reaction products separated by HPLC were collected, extracted with 1 to 1 volume of MTBE and characterized using GC–MS following the method described above.

3. Results and discussion

3.1. Linkers design and production of fusion-proteins

The sequences of the two fusion enzymes were obtained by linking the genes of CYP152B1 (SPα) to that of the Sarcosine Oxidase (SOX) through two DNA sequences corresponding to 11 amino acids. The expressed fusion protein resulted in a CYP152B1 domain at the N-terminus linked to the SOX domain at the C-terminus (Fig. 1). The first linker sequence chosen to be between the two domains is Gly-Pro-$(Gly)_7$-Pro-Gly [13]. This poly-glycine sequence is designed to be structurally flexible, as this property is desired in order to avoid restrictions in the reciprocal movement of the two enzymatic domains in the fusion system. This is also expected to preserve the natural folding of the two domains while promoting productive interactions between them [5]. The construct, called SPα-flexible-SOX, has been characterized in a recent work by our group in terms of its ability to self-regenerate hydrogen peroxide, and its catalytic performance for the conversion of fatty acids in 2-OH fatty acids was compared to the isolated wild type SPα enzyme [13]. In the present work, the SPα-flexible-SOX is used as term of comparison for the characterization of the newly designed fusion enzyme construct. The second linker sequence chosen is Glu-$(Pro)_4$-Leu-$(Pro)_4$-Glu. This was designed on the basis of a previous work in which the properties of different types of linker were investigated, and $([E/L]PPPP)_n$ containing linkers showed to effectively maintain their linear conformation in molecular dynamic experiments [25]. This behavior is due to the conformational restriction introduced by proline residues, whose side chain is covalently linked back to the backbone N, ensuring the intrinsic structural rigidity. Rigid linkers provide a separation between the fusion partners [12,25], and this may be advantageous in the case of unproductive interactions between the enzymatic domains. As we focused on considering the effect of the linker rigidity, these were designed to be similar in length (11 residues) and to lack orientation, as both are palindromes. Fig. 1 shows the template-free prediction of the

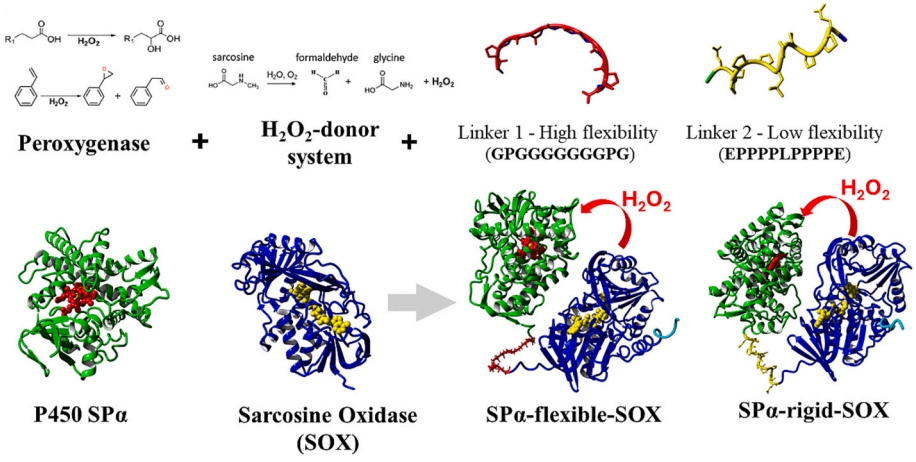

Fig. 1. Representation of the design of SPα-flexible-SOX and SPα-rigid-SOX. Sarcosine oxidase (MSOX) catalyzes the oxidation of sarcosine into glycine, formaldehyde and H_2O_2, acting as H_2O_2-donor system for the fusion enzyme catalysis. The P450 SPα peroxygenase exploits H_2O_2 for the α-hydroxylation of fatty acids or the oxidation of non-native substrates including styrene. P450 SPα and SOX structures were fused by a flexible poly-glycine linker or a rigid PPII helix linker. The P450 SPα (PDB: 3VM4) [1] and the SOX (PDB: 2GB0) [2] structures are represented as a ribbon model and colored in green and in blue respectively, the heme cofactor is colored in red, the SOX FAD cofactor is colored in yellow. The structures of the two fusion enzymes were generated by AlphaFold 2.0 [3] and colored using the same colour code. The structure of the flexible and rigid linker within the two fusion enzymes is colored in red and in yellow, respectively.

two fusion enzymes structures generated using AlphaFold 2.0 [16,26]. The detail of the two linkers structures is also showed. As expected, the poly-glycine sequence does not show a defined secondary structure and assumes a disordered loop conformation within the fusion-enzyme (SPα-flexible-SOX). On the other hand, the rigid linker displays a peculiar secondary structure, that can be classified as a left-handed poly-proline type II (PPII) helix, in which the backbone dihedral torsion angles are restricted in a fixed range ($\phi = -76°$ to $-53°$; $\psi = 133°$ to $155°$) thanks to the two poly-proline sequences [27–29]. The recombinant SPα-flexible-SOX and SPα-rigid-SOX were expressed in *E. coli* and purified using nickel chelate affinity chromatography, using a similar method compared to that already described for SPα-flexible-SOX [13]. The amount of active protein after the purification process was evaluated basing on the spectral shift of the heme-thiolate CO-bound form to 445 nm (P450 form) [13,14,21]. The protein expression and purification yield was found to be similar between the two fusion enzymes: approximately 3.57 mg/L of cell culture for SPα-flexible-SOX and 4.12 mg/L for SPα-rigid-SOX. The data indicate that the protein maturation process of both the SPα-flexible-SOX and SPα-rigid-SOX was successfully attained using *E. coli* cells as host organism.

3.2. Differential scanning calorimetry

In order to investigate the effect of the rigid linker on the fusion enzyme unfolding, differential scanning calorimetry of SPα-rigid-SOX was performed, and data are herein compared to the SPα-flexible-SOX thermogram previously reported (Fig. 2, Table 1) [13]. The experimental curves were accurately fitted using a non-two state denaturation model and deconvoluted to extrapolate the endothermal peaks associated to each denaturation transition. In order to assign each endothermal peak to one of the fusion enzyme domains (in our case the two main domains are the SPα and the SOX structures) their melting temperatures (T_M) were considered, as previously described [13]. In brief, the second endothermal peak was assigned to SOX domain on the basis of the reported melting temperature of the isolated MSOX enzyme (T_M: 64 °C) [30,31] and the first endothermal peak to SPα. According to this analysis the higher energy barrier to unfolding observed for the rigid construct was found to be almost entirely associated to the denaturation of the SPα domain, corresponding to an enthalpy value of 452 kcal/mol, equal to two times that extrapolated for the SPα domain of the flexible construct (225 kcal/mol) (Table 1). On the other hand, the ΔH associated to the SOX denaturation was comparable between SPα-rigid-SOX and SPα-flexible-SOX (respectively 313 kcal/mol and 336 kcal/mol for SPα-rigid-SOX and SPα-flexible-SOX). The higher enthalpy associated to the denaturation of the SPα-rigid-SOX suggests a stabilization of the enzyme folding-state in solution, due to the structural constraint given by the poly-proline linker. Although the T_M of each fusion protein domain did not show any significant difference between SPα-rigid-SOX and SPα-flexible-SOX, a 10 °C increase in the temperature of onset (T_{onset}) of the endothermal transition of the rigid fusion enzyme was observed (Table 1). These latter data support an increase in the thermal stability of the P450 domain within the rigid complex. Moreover, the SPα domain of the SPα-flexible-SOX showed a transition of unfolding over a range of temperature of about 30 °C (ΔT: 70–40 °C) whereas the SPα domain of the SPα-rigid-SOX completely unfolded within 15 °C (ΔT: 65–50 °C), implying a higher cooperativity of folding of the P450 domain in the rigid fusion enzyme [32]. Assessing the overall denaturation profile of the two fusion enzymes, it was found that SPα-rigid-SOX displayed a globally higher energy barrier to unfolding (765 kcal/mol for SPα-rigid-SOX and 561 for SPα-flexible-SOX). Moreover, the detection of two unfolding transitions was found to be more prominent in the SPα-rigid-SOX thermogram, indicating a better separation of the fusion enzyme functionalities and allowing an accurate recognition of the single domains denaturation. Taken together, the greater enthalpy with the increase of the T_{onset} and the higher cooperativity of the SPα folding state demonstrate the distinctive effect of the linker rigidity on the structural features of the P450 in the context of the fusion enzyme.

Table 1
Differential scanning calorimetry analysis of SPα-flexible-SOX and SPα-rigid-SOX.

SPα-flexible-SOX [13]		SPα-rigid-SOX	
T_M1	59.3 ± 0.3 °C	T_M1	57.9 ± 0.03 °C
ΔH1	224.7 ± 8.1 kcal/mol	ΔH1	452.1 ± 1.0 kcal/mol
T_M2	63.2 ± 0.02 °C	T_M2	62.8 ± 0.02 °C
ΔH2	336.4 ± 7.1 kcal/mol	ΔH2	312.7 ± 5.1 kcal/mol
T_{onset}	> 40 °C	T_{onset}	> 50 °C

Differential scanning calorimetry analysis of SPα-flexible-SOX [13] and SPα-rigid-SOX unfolding transition. Data were extrapolated by fitting the denaturation profile experimental curve using a non-two state denaturation model. T_m: melting temperature, ΔH: enthalpy, T_{onset}: temperature of onset of the denaturation transition. The denaturation transitions 1 and 2 are associated to the P450 SPα and SOX domain unfolding respectively.

3.3. Single-domains thermal stability

The thermal stability of the two enzymes within the chimeras was

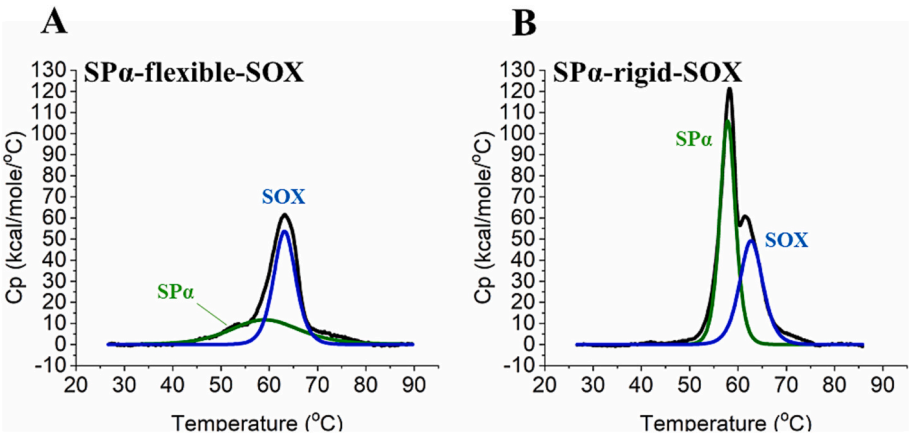

Fig. 2. Denaturation profiles of SPα-flexible-SOX [4] (A) and SPα-rigid-SOX (B) obtained by differential scanning calorimetry experiments. Black traces represent the experimental curves obtained applying a temperature gradient of 25–90 °C with a scan rate of 60 °C/h after 10 min of pre-scan equilibration, the same buffer was used also for the reference scan. The protein sample was suspended in 50 mM KPi at pH 7.4 supplemented with 10 % glycerol at a final concentration of 5 μM. Green and blue traces represent, respectively, the endothermal transition of SPα and SOX domain after the experimental curve fitting and deconvolution.

further assessed measuring the residual activity of each fusion protein functionality after a pre-incubation at a temperature ranging between 30° and 65 °C. A protein sample not pre-incubated at each temperature was used as term of comparison to calculate the residual activity of each fusion-protein domain. The SPα domain activity was estimated on the basis of the decay of the carbon monoxide binding to the heme-thiolate after incubation at increasing temperature by UV-VIS spectroscopy. The curves of the heme domain residual activity within the two fusion enzymes were accurately fitted using a Hill's like equation and the T_{50} and the decay constant (K_{decay}) were extrapolated (Fig. 3). SPα-rigid-SOX showed a higher efficiency to bind the CO at any temperature tried compared to the SPα-flexible-SOX. Moreover, the P450 domain of SPα-rigid-SOX showed a shift of the T_{50} of 5.7 °C, reaching 52.2 °C, compared to the SPα-flexible-SOX (46.5 °C). The data confirmed the increase of the thermal stability of the heme domain within the rigid complex. Moreover, the K_{decay} of the SPα domain activity within the rigid construct increased (−16.0 for SPα-rigid-SOX and − 12.3 for SPα-flexible-SOX). These latter data are in line with a higher cooperativity in the unfolding behavior of the P450 domain in the SPα-rigid-SOX. Interestingly, the analysis of the UV-VIS spectra of the fusion enzyme after thermal denaturation and CO-binding, shows the presence of a peculiar CO-bound form of the SPα absorbing at 422 nm. This species is stabilized only within the rigid construct and it can be detected up to a temperature of 60 °C, at which point the activity of the enzyme is substantially lost. On the other hand, in the SPα-flexible-SOX the Soret band at 422 nm was barely detectable at 45 °C and completely absent at 55 °C (Fig. 3-B and 3-C). To our knowledge, a similar heme iron state has never been observed for the wild-type SPα. It is known that cytochromes P450 can exist in a non-native, inactive form called P420 that shows a Soret band as ferrous–CO complex at 420 nm [33,34]. According to the experiments presented here, this non-native P420 form is detectable only after an incubation at high temperature in the SPα-rigid-SOX and not in the SPα-flexible-SOX. These data suggest the role of the poly-proline helix linker in the stabilization of the P450 domain structure during the thermal denaturation, which maintains the heme coordination even at high temperature. The SOX domain activity was estimated on the basis of the rate of production of hydrogen peroxide in presence of sarcosine (Fig. 4). In general, SOX showed a higher thermal stability compared to the SPα domain in both the fusion enzymes, maintaining the full activity at 46.5 °C, in line with the DSC data. Notably, at 52.2 °C – that is the T_{50} of the heme domain of SPα-rigid-SOX – the SOX domain showed to maintain the 100 % of activity within the rigid construct, but only the 70 % was observed for SPα-flexible-SOX under the same conditions. The data indicate a positive effect of the rigid linker also for the SOX structure, confirming the higher overall thermal stability of SPα-rigid-SOX.

3.4. Conversion of lauric acid at high temperature

High-temperature performance is a critical factor in developing fusion systems for biotechnological applications. The catalytic activity of the wild type SPα, SPα-flexible-SOX and SPα-rigid-SOX for the conversion of the P450 SPα physiological substrate lauric acid into 2-OH lauric acid was tested. The results are shown in Fig. 5, and the mass spectrometry analysis of the resulting metabolites is reported in Fig. S1. Considering the higher thermal stability of SPα-rigid-SOX observed in the previous experiments, the activity of the three enzymes was investigated at the reference temperature of 30 °C, that is typically applied for P450 SPα biocatalysis, as well as at 40 °C (Fig. 5 C). At 30° both the fusion enzymes showed an almost doubled lauric acid conversion yield

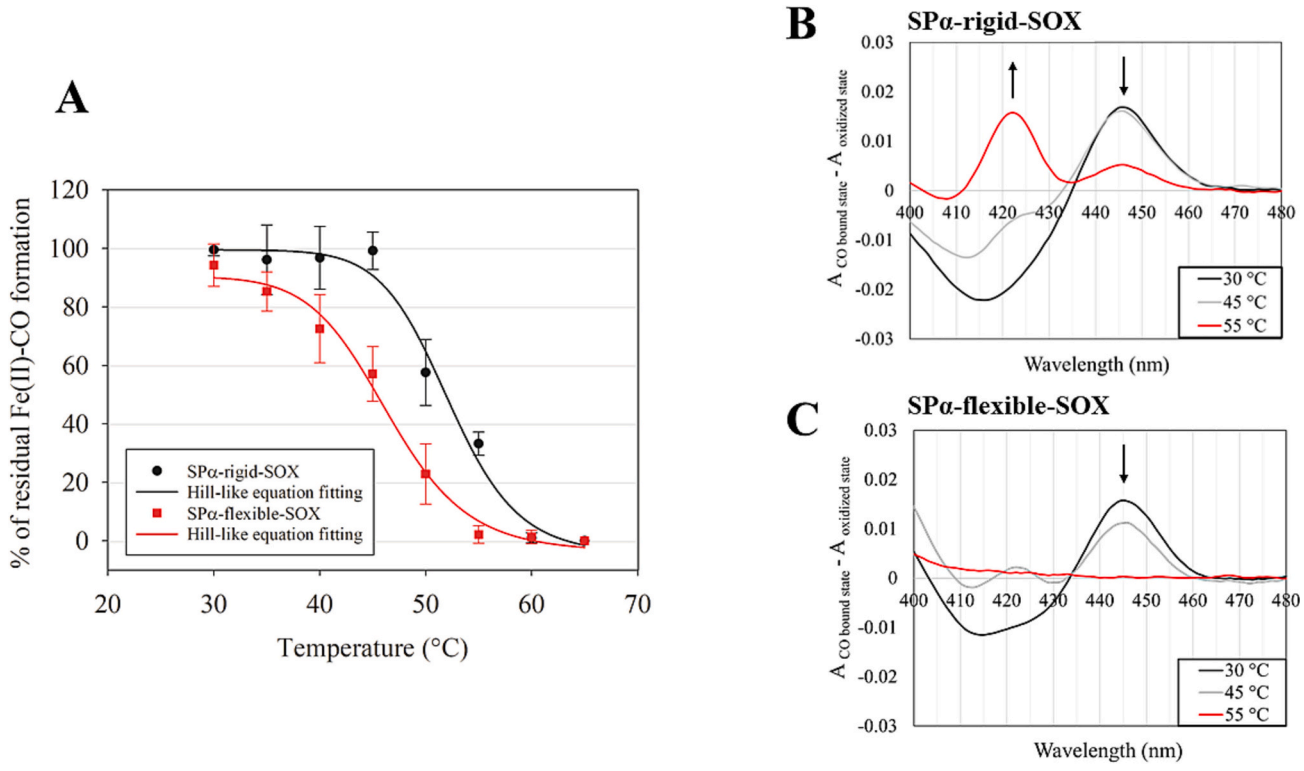

Fig. 3. Residual CO-binding experiment of SPα-rigid-SOX and SPα-flexible-SOX. (A) Trend of P450 form formation of SPα-rigid-SOX (black dots) and SPα-flexible-SOX (red squares) as a function of pre-incubation temperature. 0.2 μM of protein were incubated in KPi solution at pH 7.4 at the given temperature for 20 min. The P450 form was measured after the addition of sodium dithionite and pure CO-bubbling. All the measurements were performed at 25 °C. The percentage of residual activity was calculated basing on the total Soret shift of an identical protein sample not pre-incubated. Black and red lines represent the Hill's like equation fitting. Error bars represent the standard deviation of at least three replicates. (B, C) Difference spectra between the CO-bound form and the oxidized form of SPα-rigid-SOX (B) and SPα-flexible-SOX (C) after incubation at the three reported temperatures. SPα-rigid-SOX showed to assume a stabilized P420 form after the thermal denaturation at 55 °C.

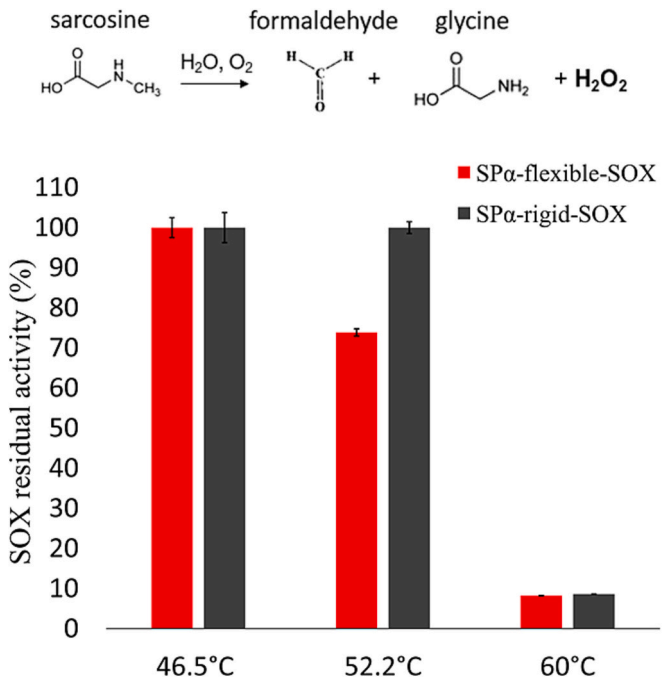

Fig. 4. Residual activity of SOX within SPα-rigid-SOX (black bars) and SPα-flexible-SOX (red bars) at different temperatures. 46.5 °C and 52.2 °C correspond to the measured T_{50} of the heme domain of SPα-flexible-SOX and SPα-rigid-SOX respectively. 7.5 nM of enzyme were mixed with 0.42 μM horseradish peroxidase (HRP), 208 μM ABTS and 42 mM sarcosine. The rate of H_2O_2 production was calculated on the basis of the $ABTS^{\bullet+}$ formation over 60 s. The percentage of residual activity was calculated on the basis of the hydrogen peroxide production rate of an identical protein sample not pre-incubated at each temperature. Error bars represent the standard deviation of at least three replicates.

compared to the isolated wild type SPα (1.2, 2.0 and 2.2 mM for wild type SPα, SPα-flexible-SOX and SPα-rigid-SOX respectively). The data indicate an overall catalytic advantage for the peroxygenase activity of SPα in the two fusion enzymes. Similar results have been reported in recent studies with different peroxygenase-H_2O_2 donor couples, showing the general advantage of self-sufficient peroxygenase systems in terms of catalytic performance compared to the isolated parent enzymes, and the crucial effect of the linker sequence choice [13,35–38]. To explain the competitive advantage of the fusion enzymes, previous works have indicated that efficient substrate delivery through adequate channeling is the primary cause of the catalytic improvement. [39,40]. Therefore, also in our case, it can be inferred that a more efficient hydrogen peroxide supply guaranteed by SOX activity is the driver for better catalysis.

Most interestingly, both SPα and SPα-flexible-SOX showed a decrease in activity at 40 °C, consistent with the thermal protein damage. On the other hand, the SPα-rigid-SOX showed an even increased lauric acid conversion, reaching 100 % yield of conversion over 1 h incubation using 5 mM substrate and 1 μM enzyme (Fig. 5 B-C). This proof-of-concept experiment demonstrates the applicability of the SPα-rigid-SOX biocatalysis at high temperature, and show that the improved thermal stability of this system can be exploited to increase the catalytic performance of the P450 SPα.

3.5. *Catalysis toward a non-physiological substrate: evaluation of styrene conversion products by SPα-SOX*

The SPα chimera activity toward non-physiological substrates was investigated using styrene as a test substrate. The largely accepted reaction mechanism of CYP152s involves the interaction of the terminal carboxylate of the physiological substrates (i.e. fatty acids) with a conserved residue of arginine at the distal side of heme [21,41,42]. The salt-bridge between the carboxylate group of the fatty acid and the guanidine group of the arginine acts as acid-base catalyst for the O—O bond cleavage of the hydrogen peroxide and the formation of Compound I. However, it was observed that P450 SPα is able to convert non-carboxylate substrates, such as styrene, in presence of a n-alkyl carboxylic acid which can act as "decoy molecule", tricking the substrate recognition of the enzyme [2,19,43,44]. Among the others carboxylic acids, wild type SPα showed a higher turnover rate for the conversion of styrene when acetate anion was used as decoy molecule [45]. In this study, a typical reaction containing SPα-rigid-SOX, sarcosine, sodium acetate and styrene was analyzed using GC–MS to evaluate the products of the conversion of styrene by the SPα chimera (Figs. 6 B, S2). SPα-rigid-SOX showed to convert styrene into styrene epoxide, phenylacetaldehyde and 2-phenylpropenal. Interestingly, the production of 2-

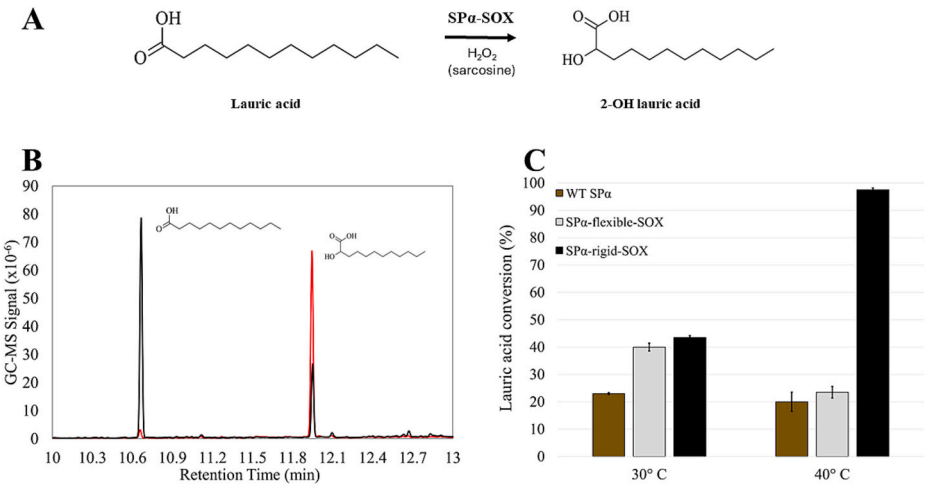

Fig. 5. Fatty acid conversion. (A) Reaction scheme represents the conversion of lauric acid into 2-OH lauric acid by SPα catalysis in presence of H_2O_2 added in solution (for wild type SPα) or produced by the SOX-dependent sarcosine oxidation (for SPα-rigid-SOX and SPα-flexible-SOX). (B) GC–MS chromatograms showing the substrate and the product detected in a typical lauric acid reaction by SPα-rigid-SOX (red curve) and SPα-flexible-SOX (black curve) performed at 40 °C. The compounds mass spectra are reported in the Fig. S1. (C) Percentage of lauric acid consumption by wild-type SPα (WT SPα, brown bars), SPα-flexible-SOX (grey bars) and SPα-rigid-SOX (black bars) catalysis performed at 30 °C or 40 °C. All reactions were performed using 1 μM of enzyme, 5 mM lauric acid, 5 mM H_2O_2 (for WT SPα) or 500 mM sarcosine (for SPα-rigid-SOX and SPα-flexible-SOX) in KPi 50 mM at pH 7.4 for 60 min. Error bars represent the standard deviation of three replicates.

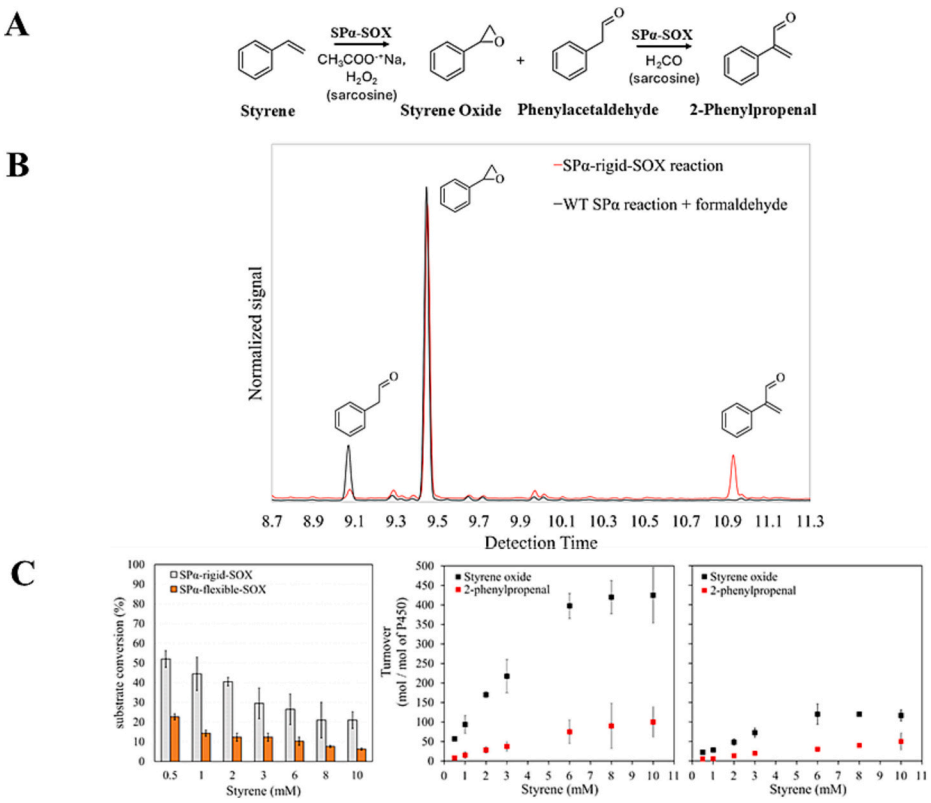

Fig. 6. Styrene conversion. (A) Reaction scheme represents the conversion of styrene into styrene oxide and phenylacetaldehyde by SPα-SOX catalysis in presence of sodium acetate and H_2O_2 (produced by the SOX-dependent sarcosine oxidation), and the subsequent conversion of phenylacetaldehyde into 2-phenylpropenal in presence of the SOX catalysis byproduct formaldehyde. (B) Magnification of the GC–MS chromatogram showing the products of a typical styrene reaction by SPα-rigid-SOX catalysis (red curve), compared to that of wild-type SPα in presence of a stoichiometric concentration of formaldehyde (black curve). Reactions were performed using 10 mM styrene and alternatively 500 mM sarcosine or 5 mM H_2O_2 and 5 mM formaldehyde in KPi 50 mM at pH 7.4 supplemented with 500 mM sodium acetate for 20 min at 30 °C. The signal was corrected to show the ratio between the different products peaks. The full chromatogram of the SPα-rigid-SOX and the peaks' mass spectra are reported in the Fig. S2. (C) Percentage of styrene consumption by SPα-rigid-SOX and SPα-flexible-SOX catalysis (left panel) and turnover of styrene oxide and 2-phenylpropenal by SPα-rigid-SOX (middle panel) and SPα-flexible-SOX (right panel). All reactions were performed using 4 μM of enzyme, styrene and 500 mM sarcosine in KPi 50 mM at pH 7.4 supplemented with 500 mM sodium acetate for 20 min at 30 °C.

phenylpropenal has never been reported as SPα catalysis product for the oxidation of styrene. Moreover, the phenylacetaldehyde production by SPα-rigid-SOX activity was almost absent compared to the wild type SPα (Fig. 6 B) [19,45]. 2-phenylpropenal (Atropaldehyde) can be produced by organic synthesis starting from phenylacetaldehyde and formaldehyde [46]. Since formaldehyde is one of the byproducts of the oxidation of sarcosine by SOX catalysis [20,47,48], the possible addition reaction of formaldehyde to phenylacetaldehyde during the SPα and SOX combined catalysis was investigated. In control experiments, when the reaction was performed using the isolated SPα (in the absence of SOX), 2-phenylpropenal was not detected, whereas the ratio between styrene oxide and phenylacetaldehyde was found to be 85/15, in line with the reported products profile for this enzyme [19,45]. The concentration of formaldehyde accumulated by the fusion enzyme reaction in excess of sarcosine was measured and resulted 5.1 ± 0.1 mM. When the same amount of formaldehyde was added in solution during the wild type SPα catalysis, the presence of 2-phenylpropenal was detected in trace amount (0.4 %), confirming that formaldehyde is involved in the formation of this byproduct. However, the significative higher formation of 2-phenylpropenal and the lower concentration of phenylacetaldehyde at the end of SPα-rigid-SOX reaction suggests that the SPα and SOX concerted catalysis positively affected the phenylacetaldehyde-formaldehyde reaction. Indeed, the data univocally indicates that the formation of 2-phenylpropenal is favored particularly in the context of the fusion enzyme. Even if the mechanism of this improved specific yield for 2-phenylpropenal within the fusion enzyme must be further elucidated, this effect can be due to the better transfer of the two intermediates of reaction, formaldehyde and phenylacetaldehyde, between the active sites of SOX and SPα respectively, leading to the increased yield of the addiction product. The fusion enzyme displayed optimized catalysis for the formation of a novel styrene oxidation product, highlighting the potential of multidomain chimeric enzymes to alter the reaction specificity of a cytochrome P450.

3.6. Styrene conversion performance

In light of the relatively poor thermal stability of styrene metabolites, in order to test the catalytic performance of SPα-rigid-SOX and SPα-flexible-SOX toward non-physiological SPα substrates, the efficiency of conversion of styrene was tested in mild conditions, employing the two enzymes catalysis at 30 °C. Both the styrene consumption at scalar concentration of substrate and the production of the two main biocatalysis products (styrene oxide and 2-phenylpropenal) were measured. Remarkably, in all the tested conditions, SPα-rigid-SOX outperformed SPα-flexible-SOX both in terms of total substrate conversion and turnover for the two products (Fig. 6 C). The extrapolated k_{cat} value of SPα-rigid-SOX for styrene conversion into styrene oxide is 36.7 ± 2.6 min-1 with a K_M of 6.7 ± 0.9 mM. The k_{cat}/K_M of SPα-rigid-SOX was found to be 3 times higher compared to SPα-flexible-SOX (k_{cat}: 9.0 ± 0.78 and K_M: 4.8 ± 0.91). When the enzyme was used at its full potential, in presence of an excess of substrate (10 mM of styrene), SPα-rigid-SOX showed to consume the 21 % of styrene, versus the 6 % of the flexible construct. The turnover number of SPα-rigid-SOX for styrene oxide production was 425 μmoles/μmole of enzyme, compared to 117

μmoles/μmole of enzyme of the flexible construct. The styrene oxide/2-phenylpropenal ratio was found to be approximately constant at the increase of the substrate concentration and similar between SPα-rigid-SOX and SPα-flexible-SOX, respectively 85/15 and 80/20 (Fig. 6 C). Overall, these data demonstrate that also under mild reaction conditions, SPα-rigid-SOX exhibits better catalytic performances compared to SPα-flexible-SOX for the conversion of a non-physiological substrate. In mild conditions the higher thermal stability of SPα-rigid-SOX is reasonably not involved in the increase of the activity, the data show the beneficial effect of the rigid linker on the combined catalysis of the SPα and SOX, regardless the applied temperature during biocatalysis.

4. Conclusions

The *Molecular Lego* approach is a powerful method for the rational design of artificial chimeric multidomain enzymes. Over the years, this strategy has delivered remarkable results [11,39,49–52], demonstrating that the *chimerization* of non-physiological redox partners is a suitable strategy to design self-sufficient biocatalysts. More recently, self-sufficient peroxygenase chimeras including CYP116B5-SOX [7,8] and $OleT_{Je}$-AldO [3] were also studied and showed positive effects on the P450 catalysis and stability. The role of the domains-linker has proven to be of fundamental importance to improve the stability in solution and the overall performance of fusion systems of different design [12,25,53–55]. In the present study, the investigation is directed to explore how the rigidity of the linker affects the properties of an artificial peroxygenase fusion system. Although usually a flexible linker is the "safer choice" for the design of fusion enzymes, since it is supposed to not affect the native folding and the reciprocal positioning of the enzymatic domains [12], the data herein presented demonstrate that the use of a rigid linker may positively affect the stabilization of the fusion system. The increase in enthalpy, T_{onset} (Fig. 2, Table 1), T_{50} (Fig. 3-A), and folding cooperativity observed in SPα-rigid-SOX during DSC and residual activity experiments clearly indicate the enhanced protein stability compared to SPα-flexible-SOX. Additionally, a stabilized P420 form of SPα was observed exclusively in the SPα-rigid-SOX construct (Fig. 3-B and -C). The two fusion enzymes showed a similar activity for lauric acid conversion at 30 °C, whereas the SPα-rigid-SOX show an increased activity at 40 °C (Fig. 5). This effect is probably due to the low solubility of the fatty acid at a relatively low temperature, which limits the enzyme turnover. SPα-rigid-SOX can be exploited at higher operating temperature, enhancing both the availability of the fatty acid and the enzyme substrate encounter probability. Furthermore, SPα-rigid-SOX displayed higher K_{cat}/K_M even for styrene oxidation indicating that there is no evident trade-off between enzyme activity and stability. A possible explanation is that rigid linker fixes the reciprocal positions between the two domains and favors productive catalysis. On the other hand, the rigid linker does not impair the required intra-domain plasticity required for catalysis, implying that no major conformational changes are expected to occur for the single domains during catalysis.

Taken together, these findings highlight the significant stabilizing effect of the PPII helix linker on the fusion system structure, also evidencing that the combined catalysis of SPα and SOX is more efficient in the context of the SPα-rigid-SOX. This effect is most probably due to both the improved stability of the fusion system and the better hydrogen peroxide transfer between the two enzymatic domains. Although biocatalysis studies on a broader range of substrates is required, we conclude that this work represents a step forward in the field of knowledge-based design of self-sufficient fusion enzymes, highlighting their potential in the field of biotechnology and synthetic biology.

CRediT authorship contribution statement

Daniele Giuriato: Writing – original draft, Visualization, Formal analysis, Data curation, Conceptualization. **Gianluca Catucci:** Writing – review & editing, Formal analysis, Data curation, Conceptualization. **Danilo Correddu:** Visualization, Formal analysis, Data curation, Conceptualization. **Gianfranco Gilardi:** Writing – review & editing, Supervision, Resources, Project administration, Funding acquisition, Conceptualization.

Declaration of competing interest

The authors declare that they have no known competing financial interests or personal relationships that could have appeared to influence the work reported in this paper.

Acknowledgements

We thank Professor Yoshihito Watanabe for having kindly gifted the vector harboring the SPα gene.

Appendix A. Supplementary data

Supplementary data to this article can be found online at https://doi.org/10.1016/j.ijbiomac.2025.145497.

Data availability

All data generated or analyzed during this study are included in this published article [and its supplementary information files].

References

[1] R. Bernhardt, V.B. Urlacher, Cytochromes P450 as promising catalysts for biotechnological application: chances and limitations, Appl. Microbiol. Biotechnol. 98 (2014) 6185–6203, https://doi.org/10.1007/s00253-014-5767-7.
[2] O. Shoji, Y. Watanabe, Peroxygenase reactions catalyzed by cytochromes P450, J. Biol. Inorg. Chem. 19 (2014) 529–539, https://doi.org/10.1007/s00775-014-1106-9.
[3] S. Matthews, K.L. Tee, N.J. Rattray, K.J. McLean, D. Leys, D.A. Parker, R. T. Blankley, A.W. Munro, Production of alkenes and novel secondary products by P450 OleTJE using novel H2O2-generating fusion protein systems, FEBS Lett. 591 (2017) 737–750, https://doi.org/10.1002/1873-3468.12581.
[4] P. Gomez de Santos, S. Lazaro, J. Viña-Gonzalez, M.D. Hoang, I. Sánchez-Moreno, A. Glieder, F. Hollmann, M. Alcalde, Evolved peroxygenase–aryl alcohol oxidase fusions for self-sufficient oxyfunctionalization reactions, ACS Catal. 10 (2020) 13524–13534, https://doi.org/10.1021/acscatal.0c03029.
[5] Y. Ma, N. Zhang, G. Vernet, S. Kara, Design of fusion enzymes for biocatalytic applications in aqueous and non-aqueous media, Front. Bioeng. Biotechnol. 10 (2022), https://doi.org/10.3389/fbioe.2022.944226 (accessed February 5, 2024).
[6] Á. Mourelle-Insua, F.S. Aalbers, I. Lavandera, V. Gotor-Fernández, M.W. Fraaije, What to sacrifice? Fusions of cofactor regenerating enzymes with Baeyer-Villiger monooxygenases and alcohol dehydrogenases for self-sufficient redox biocatalysis, Tetrahedron 75 (2019) 1832–1839, https://doi.org/10.1016/j.tet.2019.02.015.
[7] D. Giuriato, G. Catucci, D. Correddu, G.D. Nardo, G. Gilardi, CYP116B5-SOX: an artificial peroxygenase for drug metabolites production and bioremediation, Biotechnol. J. 19 (2024) 2300664, https://doi.org/10.1002/biot.202300664.
[8] D. Correddu, G. Catucci, D. Giuriato, G. Di Nardo, A. Ciaramella, G. Gilardi, Catalytically self-sufficient CYP116B5: domain switch for improved peroxygenase activity, Biotechnol. J. 18 (2023) 2200622, https://doi.org/10.1002/biot.202200622.
[9] F. de M. García-Paz, S. Del Moral, S. Morales-Arrieta, M. Ayala, L.G. Treviño-Quintanilla, C. Olvera-Carranza, Multidomain chimeric enzymes as a promising alternative for biocatalysts improvement: a minireview, Mol. Biol. Rep. 51 (2024) 410, https://doi.org/10.1007/s11033-024-09332-9.
[10] G. Catucci, A. Ciaramella, G. Di Nardo, C. Zhang, S. Castrignanò, G. Gilardi, Molecular lego of human cytochrome P450: the key role of heme domain flexibility for the activity of the chimeric proteins, Int. J. Mol. Sci. 23 (2022) 3618, https://doi.org/10.3390/ijms23073618.
[11] G. Gilardi, Y.T. Meharenna, G.E. Tsotsou, S.J. Sadeghi, M. Fairhead, S. Giannini, Molecular lego: design of molecular assemblies of P450 enzymes for nanobiotechnology, Biosens. Bioelectron. 17 (2002) 133–145, https://doi.org/10.1016/s0956-5663(01)00286-x.
[12] X. Chen, J.L. Zaro, W.-C. Shen, Fusion protein linkers: property, design and functionality, Adv. Drug Deliv. Rev. 65 (2013) 1357–1369, https://doi.org/10.1016/j.addr.2012.09.039.
[13] D. Giuriato, D. Correddu, G. Catucci, G. Di Nardo, C. Bolchi, M. Pallavicini, G. Gilardi, Design of a H2O2-generating P450SPα fusion protein for high yield fatty acid conversion, Protein Sci. 31 (2022) e4501, https://doi.org/10.1002/pro.4501.
[14] I. Matsunaga, N. Yokotani, O. Gotoh, E. Kusunose, M. Yamada, K. Ichihara, Molecular cloning and expression of fatty acid alpha-hydroxylase from

Sphingomonas paucimobilis, J. Biol. Chem. 272 (1997) 23592–23596, https://doi.org/10.1074/jbc.272.38.23592.
[15] Y. Jiang, W. Peng, Z. Li, C. You, Y. Zhao, D. Tang, B. Wang, S. Li, Unexpected reactions of α,β-unsaturated fatty acids provide insight into the mechanisms of CYP152 peroxygenases, Angew. Chem. Int. Ed. 60 (2021) 24694–24701, https://doi.org/10.1002/anie.202111163.
[16] J. Jumper, R. Evans, A. Pritzel, T. Green, M. Figurnov, O. Ronneberger, K. Tunyasuvunakool, R. Bates, A. Žídek, A. Potapenko, A. Bridgland, C. Meyer, S.A. A. Kohl, A.J. Ballard, A. Cowie, B. Romera-Paredes, S. Nikolov, R. Jain, J. Adler, T. Back, S. Petersen, D. Reiman, E. Clancy, M. Zielinski, M. Steinegger, M. Pacholska, T. Berghammer, S. Bodenstein, D. Silver, O. Vinyals, A.W. Senior, K. Kavukcuoglu, P. Kohli, D. Hassabis, Highly accurate protein structure prediction with AlphaFold, Nature 596 (2021) 583–589, https://doi.org/10.1038/s41586-021-03819-2.
[17] C.J. Williams, J.J. Headd, N.W. Moriarty, M.G. Prisant, L.L. Videau, L.N. Deis, V. Verma, D.A. Keedy, B.J. Hintze, V.B. Chen, S. Jain, S.M. Lewis, W.B. Arendall, J. Snoeyink, P.D. Adams, S.C. Lovell, J.S. Richardson, D.C. Richardson, MolProbity: more and better reference data for improved all-atom structure validation, Protein Sci. 27 (2018) 293–315, https://doi.org/10.1002/pro.3330.
[18] V.B. Chen, I.W. Davis, D.C. Richardson, KING (Kinemage, next generation): a versatile interactive molecular and scientific visualization program, Protein Sci. 18 (2009) 2403–2409, https://doi.org/10.1002/pro.250.
[19] T. Fujishiro, O. Shoji, N. Kawakami, T. Watanabe, H. Sugimoto, Y. Shiro, Y. Watanabe, Chiral-substrate-assisted Stereoselective epoxidation catalyzed by H2O2-dependent cytochrome P450SPα, Chem. Asian J. 7 (2012) 2286–2293, https://doi.org/10.1002/asia.201200250.
[20] P. Trickey, M.A. Wagner, M.S. Jorns, F.S. Mathews, Monomeric sarcosine oxidase: structure of a covalently flavinylated amine oxidizing enzyme, Structure 7 (1999) 331–345, https://doi.org/10.1016/S0969-2126(99)80043-4.
[21] T. Fujishiro, O. Shoji, S. Nagano, H. Sugimoto, Y. Shiro, Y. Watanabe, Crystal structure of H2O2-dependent cytochrome P450SPα with its bound fatty acid substrate, J. Biol. Chem. 286 (2011) 29941–29950, https://doi.org/10.1074/jbc.M111.245225.
[22] G. Catucci, D. Aramini, S.J. Sadeghi, G. Gilardi, Ligand stabilization and effect on unfolding by polymorphism in human flavin-containing monooxygenase 3, Int. J. Biol. Macromol. 162 (2020) 1484–1493, https://doi.org/10.1016/j.ijbiomac.2020.08.032.
[23] C. Gao, G. Catucci, S. Castrignanò, G. Gilardi, S.J. Sadeghi, Inactivation mechanism of N61S mutant of human FMO3 towards trimethylamine, Sci. Rep. 7 (2017) 14668, https://doi.org/10.1038/s41598-017-15224-9.
[24] E.N. Kadnikova, N.M. Kostić, Oxidation of ABTS by hydrogen peroxide catalyzed by horseradish peroxidase encapsulated into sol–gel glass.: effects of glass matrix on reactivity, J. Mol. Catal. B Enzym. 18 (2002) 39–48, https://doi.org/10.1016/S1381-1177(02)00057-7.
[25] P.J. Bakkes, J.L. Riehm, T. Sagadin, A. Rühlmann, P. Schubert, S. Biemann, M. Girhard, M.C. Hutter, R. Bernhardt, V.B. Urlacher, Engineering of versatile redox partner fusions that support monooxygenase activity of functionally diverse cytochrome P450s, Sci. Rep. 7 (2017) 9570, https://doi.org/10.1038/s41598-017-10075-w.
[26] M. Mirdita, K. Schütze, Y. Moriwaki, L. Heo, S. Ovchinnikov, M. Steinegger, ColabFold: making protein folding accessible to all, Nat. Methods 19 (2022) 679–682, https://doi.org/10.1038/s41592-022-01488-1.
[27] A.A. Adzhubei, M.J. Sternberg, Left-handed polyproline II helices commonly occur in globular proteins, J. Mol. Biol. 229 (1993) 472–493, https://doi.org/10.1006/jmbi.1993.1047.
[28] A.A. Adzhubei, M.J.E. Sternberg, A.A. Makarov, Polyproline-II helix in proteins: structure and function, J. Mol. Biol. 425 (2013) 2100–2132, https://doi.org/10.1016/j.jmb.2013.03.018.
[29] B.J. Stapley, T.P. Creamer, A survey of left-handed polyproline II helices, Protein Sci. 8 (1999) 587–595, https://doi.org/10.1110/ps.8.3.587.
[30] Y. Tong, Y. Xin, H. Yang, L. Zhang, W. Wang, Efficient improvement on stability of sarcosine oxidase via poly-lysine modification on enzyme surface, Int. J. Biol. Macromol. 67 (2014) 140–146, https://doi.org/10.1016/j.ijbiomac.2014.03.015.
[31] Y. Xin, M. Zheng, Q. Wang, L. Lu, L. Zhang, Y. Tong, W. Wang, Structural and catalytic alteration of sarcosine oxidase through reconstruction with coenzyme-like ligands, J. Mol. Catal. B Enzym. 133 (2016) S250–S258, https://doi.org/10.1016/j.molcatb.2017.01.011.
[32] V. Muñoz, L.A. Campos, M. Sadqi, Limited cooperativity in protein folding, Curr. Opin. Struct. Biol. 36 (2016) 58–66, https://doi.org/10.1016/j.sbi.2015.12.001.
[33] Y.-W. Lin, J. Wang, Structure and function of heme proteins in non-native states: a mini-review, J. Inorg. Biochem. 129 (2013) 162–171, https://doi.org/10.1016/j.jinorgbio.2013.07.023.
[34] Y. Ichikawa, T. Yamano, The role of the hydrophobic bonding in P-450 and the effect of organic compounds on the conversion of P-450 to P-420, Biochim. Biophys. Acta Protein Struct. 147 (1967) 518–525, https://doi.org/10.1016/0005-2795(67)90011-6.
[35] S. Matthews, J.D. Belcher, K.L. Tee, H.M. Girvan, K.J. McLean, S.E.J. Rigby, C. W. Levy, D. Leys, D.A. Parker, R.T. Blankley, A.W. Munro, Catalytic determinants of alkene production by the cytochrome P450 peroxygenase OleTJE*, J. Biol. Chem. 292 (2017) 5128–5143, https://doi.org/10.1074/jbc.M116.762336.
[36] P. Gomez de Santos, S. Lazaro, J. Viña-Gonzalez, M.D. Hoang, I. Sánchez-Moreno, A. Glieder, F. Hollmann, M. Alcalde, Evolved peroxygenase–aryl alcohol oxidase fusions for self-sufficient oxyfunctionalization reactions, ACS Catal. 10 (2020) 13524–13534, https://doi.org/10.1021/acscatal.0c03029.
[37] J. Carro, E. Fernández-Fueyo, C. Fernández-Alonso, J. Cañada, R. Ullrich, M. Hofrichter, M. Alcalde, P. Ferreira, A.T. Martínez, Self-sustained enzymatic cascade for the production of 2,5-furandicarboxylic acid from 5-methoxymethylfurfural, Biotechnol. Biofuels 11 (2018) 86, https://doi.org/10.1186/s13068-018-1091-2.
[38] F.A.R. Hardiyanti Oktavia, N.A. Nguyen, C.M. Park, G.S. Cha, T.H.H. Nguyen, C.-H. Yun, CYP102A1 peroxygenase catalyzed reaction via in situ H2O2 generation, J. Inorg. Biochem. 242 (2023) 112165, https://doi.org/10.1016/j.jinorgbio.2023.112165.
[39] D.T. Monterrey, I. Ayuso-Fernández, I. Oroz-Guinea, E. García-Junceda, Design and biocatalytic applications of genetically fused multifunctional enzymes, Biotechnol. Adv. 60 (2022) 108016, https://doi.org/10.1016/j.biotechadv.2022.108016.
[40] Y. Zhang, J. Liu, G. Hu, X. Hu, J. Yang, H. Zhang, Fusion enzyme design based on the "channelization" cascade theory and homogenous dextran product improvement, Int. J. Biol. Macromol. 222 (2022) 652–660, https://doi.org/10.1016/j.ijbiomac.2022.09.222.
[41] D.-S. Lee, A. Yamada, H. Sugimoto, I. Matsunaga, H. Ogura, K. Ichihara, S. Adachi, S.-Y. Park, Y. Shiro, Substrate recognition and molecular mechanism of fatty acid hydroxylation by cytochrome P450 from Bacillus subtilis: crystallographic, spectroscopic, and mutational studies*, J. Biol. Chem. 278 (2003) 9761–9767, https://doi.org/10.1074/jbc.M211575200.
[42] H.M. Girvan, H. Poddar, K.J. McLean, D.R. Nelson, K.A. Hollywood, C.W. Levy, D. Leys, A.W. Munro, Structural and catalytic properties of the peroxygenase P450 enzyme CYP152K6 from Bacillus methanolicus, J. Inorg. Biochem. 188 (2018) 18–28, https://doi.org/10.1016/j.jinorgbio.2018.08.002.
[43] O. Shoji, T. Fujishiro, H. Nakajima, M. Kim, S. Nagano, Y. Shiro, Y. Watanabe, Hydrogen peroxide dependent monooxygenations by tricking the substrate recognition of cytochrome P450BSbeta, Angew. Chem. Int. Ed. Eng. 46 (2007) 3656–3659, https://doi.org/10.1002/anie.200700068.
[44] T. Fujishiro, O. Shoji, Y. Watanabe, Non-covalent modification of the active site of cytochrome P450 for inverting the stereoselectivity of monooxygenation, Tetrahedron Lett. 52 (2011) 395–397, https://doi.org/10.1016/j.tetlet.2010.11.048.
[45] H. Onoda, O. Shoji, Y. Watanabe, Acetate anion-triggered peroxygenation of non-native substrates by wild-type cytochrome P450s, Dalton Trans. 44 (2015) 15316–15323, https://doi.org/10.1039/c5dt00797f.
[46] Q. Wu, J. Guan, Y. Yu, C. Chen, Y. Wu, Honey Aroma Compound and Preparation Method Thereof, CN116120179A, 2023.
[47] M.A. Wagner, M.S. Jorns, Monomeric sarcosine oxidase: 2. Kinetic studies with sarcosine, alternate substrates, and a substrate analogue, Biochemistry 39 (2000) 8825–8829, https://doi.org/10.1021/bi000350y.
[48] M.A. Wagner, P. Trickey, Z.W. Chen, F.S. Mathews, M.S. Jorns, Monomeric sarcosine oxidase: 1. Flavin reactivity and active site binding determinants, Biochemistry 39 (2000) 8813–8824, https://doi.org/10.1021/bi000349z.
[49] S.J. Sadeghi, G. Gilardi, Chimeric P450 enzymes: activity of artificial redox fusions driven by different reductases for biotechnological applications, Biotechnol. Appl. Biochem. 60 (2013) 102–110, https://doi.org/10.1002/bab.1086.
[50] G. Catucci, A. Ciaramella, G. Di Nardo, C. Zhang, S. Castrignanò, G. Gilardi, Molecular lego of human cytochrome P450: the key role of heme domain flexibility for the activity of the chimeric proteins, IJMS 23 (2022) 3618, https://doi.org/10.3390/ijms23073618.
[51] S.J. Sadeghi, Y.T. Meharenna, A. Fantuzzi, F. Valetti, G. Gilardi, Engineering artificial redox chains by molecular 'Lego,', Faraday Discuss. 116 (2000) 135–153, https://doi.org/10.1039/b003180l.
[52] S. Castrignanò, S. D'Avino, G. Di Nardo, G. Catucci, S.J. Sadeghi, G. Gilardi, Modulation of the interaction between human P450 3A4 and *B. megaterium* reductase *via* engineered loops, Biochim. Biophys. Acta, Proteins Proteomics 1866 (2018) 116–125, https://doi.org/10.1016/j.bbapap.2017.07.009.
[53] D. Degregorio, S. D'Avino, S. Castrignanò, G. Di Nardo, S.J. Sadeghi, G. Catucci, G. Gilardi, Human cytochrome P450 3A4 as a biocatalyst: effects of the engineered linker in modulation of coupling efficiency in 3A4-BMR chimeras, Front. Pharmacol. 8 (2017), https://doi.org/10.3389/fphar.2017.00121.
[54] S. Castrignanò, G. Di Nardo, S.J. Sadeghi, G. Gilardi, Influence of inter-domain dynamics and surrounding environment flexibility on the direct electrochemistry and electrocatalysis of self-sufficient cytochrome P450 3A4-BMR chimeras, J. Inorg. Biochem. 188 (2018) 9–17, https://doi.org/10.1016/j.jinorgbio.2018.08.003.
[55] V.R. Dodhia, A. Fantuzzi, G. Gilardi, Engineering human cytochrome P450 enzymes into catalytically self-sufficient chimeras using molecular Lego, J. Biol. Inorg. Chem. 11 (2006) 903–916, https://doi.org/10.1007/s00775-006-0144-3.